

The lattice constants of WO_3 calculated from Debye lines are plotted in Fig. 2, in which it is seen that a and b expand linearly with temperature in the orthorhombic region up to about 700°C , where an abrupt phase change occurs and the crystal becomes tetragonal, resulting in $a=b$. The lattice constant c shows a similar linearity in both phases, accompanying a discontinuous

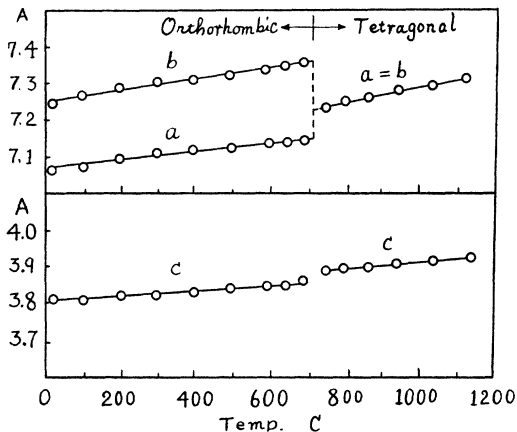


FIG. 2. Lattice constants vs temperature curve of WO_3 .

change at the transition temperature, which is, however, considerably smaller than the others. Above the transition temperature, the tetragonal lattice persists up to about 1100°C . It is uncertain at the present stage, however, whether or not WO_3 has another phase change (tetragonal \rightleftharpoons cubic) above this temperature.

It has been observed, by the dilatometer and specific heat measurements recently performed by us, that there exists a sharp contraction in volume and a fairly large energy change at about 720°C . Detailed x-ray studies to detect the minute change in the neighborhood of the transitional region by means of a back reflection method are now in progress.

The disappearance of the domain patterns at about 700°C when viewed parallel to the c -axis under the microscope may be explained easily by considering that twinning planes $\{110\}$ disappear, since the lattice parameters a and b coincide with each other. Dielectric studies will be required to reveal the ferroelectric transition of this crystal at about 720°C , but they will be exceedingly difficult on account of its semiconductive properties at higher temperatures.

The details of the investigation will be published elsewhere.

The authors wish to express their sincere thanks to Professor S. Miyake for his encouragement in the course of the study, and also to Mr. S. Sawada for his kind information.

¹ R. Ueda and T. Ichinokawa, Phys. Rev. **80**, 1106 (1950).

² S. Sawada (unpublished).

Cloud-Chamber Analysis of Stopped Particles in the Sea-Level Cosmic Radiation*

G. M. NONNEMAKER AND J. C. STREET
Lyman Laboratory of Physics, Harvard University,
Cambridge, Massachusetts
(Received March 26, 1951)

A WILSON cloud chamber beneath a filter of 119 g cm^{-2} lead plus 21 g cm^{-2} lead-equivalent and above an absorber of 81 g cm^{-2} lead plus 7 g cm^{-2} lead-equivalent was expanded by an anticoincidence arrangement which selected particles stopping in

the absorber (see Fig. 1). The momentum was determined from the track curvature in a magnetic field of about 4300 gauss. The specific ionization was estimated from the density of droplets along the track as compared with minimum ionization tracks. From these two quantities, particles occurring singly were identified as electrons, mesons, or protons. Although pi-mesons were indistinguishable from mu-mesons in this experiment, as is seen

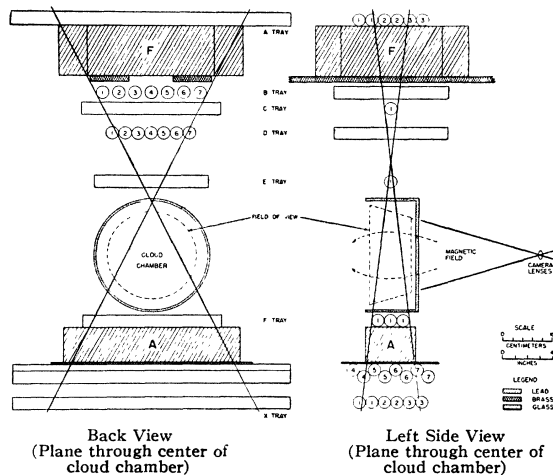


FIG. 1. Experimental arrangement. The cloud chamber was expanded by the event (A B_n C D_n E F-X).

below, the momentum cutoff indicates that the mesons are predominantly mu-mesons, as is expected.

A total of 348 pictures were taken at an average rate of 0.0159 count/min. Of these, 227 were mu-mesons, 10 were dense tracks with momenta greater than $250 \text{ Mev}/c$, 23 were energetic particles which failed to trigger the anticoincidence tray beneath the absorber, 15 were single electrons with momenta less than $70 \text{ Mev}/c$, and 73 were other electronic events such as showers and knock-on processes which triggered the proper sequence of counters.

By assuming that the telescope counting rate of (0.503 ± 0.003) count/min is due entirely to the hard component,¹ the absolute intensity of mesons stopping within the differential range interval of this experiment was found to be $(3.26 \pm 0.23) \times 10^{-6} \text{ g}^{-1} \text{ sec}^{-1} \text{ sterad}^{-1}$ (air-equivalent) for mesons with a range of 115 g cm^{-2} (air-equivalent).^{2,3} The intensity has been corrected by +7 percent for mesons lost by scattering and magnetic deflection, by +3 percent for the difference in angular distribution between the hard component and the slow mesons,² by -10 percent for the effective increase of the lead absorber as a result of multiple scattering,⁴ and by -8 percent for the inclusion of single electrons which could not be distinguished from mu-mesons in the momentum interval $70 \text{ Mev}/c$ to $160 \text{ Mev}/c$.

The ratio of positive to negative mesons stopping in the absorber was 0.94 ± 0.07 .

The observed differential distribution in momentum of the stopped mesons (see Fig. 2) had a low intensity tail extending beyond the expected vertical cutoff of $216 \text{ Mev}/c$ to about $400 \text{ Mev}/c$ probably as a result of multiple scattering in the absorber. The upper cutoff in momentum as determined from this distribution gave a meson mass of 220 ± 12 electron masses. A mass determination was not made from the lower cutoff in momentum because the thickness of material penetrated was not known to better than 10 percent.

The 10 particles which formed dense tracks were all positively charged. One of them was identified as an alpha-particle (or heavier nucleus). The remaining nine particles had mass values which ranged from 900 to 2000 electron masses. However, since the

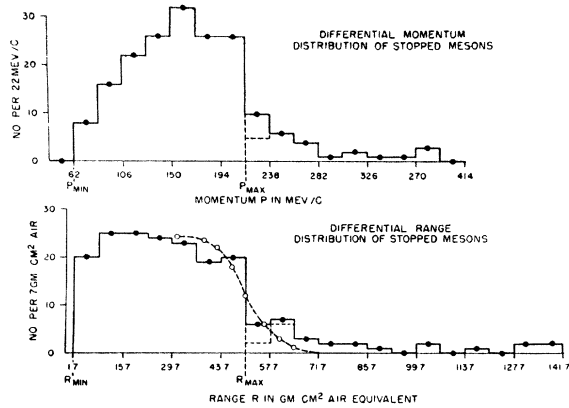


FIG. 2. Momentum and range distribution of stopped mesons. The range distribution was obtained by transforming the momentum distribution under the assumption of a mu-meson mass of 216 electron masses.

errors were difficult to evaluate, all that can be said at present is that they are probably protons. If the technique can be significantly improved, a similar experiment will be undertaken in order to obtain more accurate mass determinations.

* This work was supported in part by the joint program of the ONR and AEC.

¹ B. Rossi, *Revs. Modern Phys.* **20**, 537 (1948).

² W. L. Kraushaar, *Phys. Rev.* **76**, 1045 (1949).

³ L. Germain, *Phys. Rev.* **80**, 616 (1950).

⁴ H. P. Koenig, *Phys. Rev.* **69**, 590 (1946).

Theory of Antiferromagnetic Resonance

C. KITTEL

Bell Telephone Laboratories, Murray Hill, New Jersey

(Received April 2, 1951)

WE calculate the frequencies associated with magnetic dipole transitions in an antiferromagnetic crystal, extending to dynamic effects the Van Vleck theory of antiferromagnetism, which works remarkably well for static effects. The model is that of two sublattices of magnetization \mathbf{M}_1 , \mathbf{M}_2 oppositely directed and each of magnitude M_s . The calculation given here is classical; a quantum calculation following the method used by Van Vleck¹ in ferromagnetic resonance has been made and will be discussed in a subsequent publication.

The exchange forces are treated as molecular fields $\mathbf{H}_1 = -\lambda\mathbf{M}_2$, $\mathbf{H}_2 = -\lambda\mathbf{M}_1$ acting on the sublattices 1 and 2. It is known that there are preferred directions of orientation in antiferromagnetic crystals, and in analogy to ferromagnetism we introduce an anisotropy energy density constant K to describe the energy involved in turning both spin systems together relative to the crystal lattice. We may then, for small deflections, say that there is an anisotropy field $H_A = K/M_s$ acting on each sublattice. We take the static field H_0 and the preferred axis to be in the z -direction. We suppose that the crystal consists of a single domain and is spherical in shape, so that demagnetizing effects do not enter.

The equations of motion with a transverse rf field are

$$\begin{aligned} d\mathbf{M}_1/dt &= \gamma\mathbf{M}_1 \times [(H^x - \lambda M_2^z)\mathbf{i} \\ &\quad + (H^y - \lambda M_2^y)\mathbf{j} + (H_0 + H_A + H_E)\mathbf{k}]; \\ d\mathbf{M}_2/dt &= \gamma\mathbf{M}_2 \times [(H^x - \lambda M_1^z)\mathbf{i} \\ &\quad + (H^y - \lambda M_1^y)\mathbf{j} + (H_0 - H_A - H_E)\mathbf{k}]; \end{aligned}$$

here $H_E = \lambda M_s = \lambda M_1^z = -\lambda M_2^z$. Defining $M^- = M_x - jM_y$, $H^- = H_x - jH_y$, we solve for the susceptibility:

$$\begin{aligned} \chi^- &= M^-/H^- = 2\gamma^2 M_s H_A / (\omega - \omega_0)^2; \\ \omega_0/\gamma &= H_0 \pm [H_A(H_A + 2H_E)]^{1/2}. \end{aligned} \quad (1)$$

Note that H_E enters only if $H_A \neq 0$. For $H_0 = 0$ and $H_A \ll H_E$, the

zero field splitting is $\omega_0 \cong \gamma(2H_A H_E)^{1/2} = \gamma(2K\lambda)^{1/2}$. The two frequencies in Eq. (1) correspond to different directions of circular polarization, and a linearly polarized rf field will excite both precessional modes. In polycrystalline specimens the line widths will be at least of the order of H_0 , as only the component of the static field parallel to the domain axis is fully effective.

In the common antiferromagnetics such as MnO, MnF₂, FeO, and Cr₂O₃, we may estimate $H_A \sim 10^3$ oersteds and $H_E \sim 10^6$ oersteds. Then $(2H_A H_E)^{1/2} \sim 5 \times 10^4$ oersteds and $\omega_0 \sim 5 \text{ cm}^{-1}$, which is higher than the experimental frequency 0.3 cm^{-1} used by Maxwell² *et al.* and Hutchison.³ The low experimental frequency is the reason we suggest to explain the observed extinction of the spin resonance absorption lines in antiferromagnetic crystals on cooling below the Curie temperature. It would be valuable to work in intense magnetic fields to pull one of the frequencies into the usual range, or else to work at millimeter wavelengths.

We note that the anisotropy energy may be quite high even in cubic antiferromagnetics containing Mn²⁺ ions in a ⁶S ground state. Consider a simple-minded model: the Kramers superexchange interaction⁴ connecting Mn ions in MnO depends on the overlap of the wave functions of electrons on the Mn and O ions. With an admixture of orbital moment the overlap depends on the spin direction. The order of magnitude of the anisotropy energy per ion on this model may be estimated as $\sim |g-2|k\Theta$; for $\Delta g \sim 10^{-2}$ and $k\Theta \sim 5 \times 10^2 \text{ cm}^{-1}$ the anisotropy field can be as high as 10^4 oersteds.

With ferrite-type ferromagnetism, according to the Néel theory, we may set $M_1^z = M_s$; $M_2^z = -(1-\eta)M_s$. The observed saturation magnetization is $M_1^z + M_2^z = \eta M_s$. We let $H_E = \lambda M_s$, and suppose for simplicity that H_A has the same value for both sublattices. We find

$$\omega/\gamma = H_0 - (\eta H_E/2) \pm [(\eta H_E/2)^2 + H_E H_A (2-\eta) + H_A^2]^{1/2}.$$

The over-all anisotropy field deduced from static deflections at small angles will differ in ferrites from that deduced from microwave resonance experiments by a fractional amount $\propto H_A/H_E\eta$, which may usually be neglected. The difference should be detectable in weakly magnetic zinc ferrites.

¹ J. H. Van Vleck, *Phys. Rev.* **78**, 266 (1950).

² Trounson, Bleil, and Maxwell, *Phys. Rev.* **79**, 226 (1950); L. R. Maxwell, talk at Pittsburgh meeting APS, March 1951.

³ C. A. Hutchison, private communication.

⁴ P. W. Anderson, *Phys. Rev.* **79**, 350 (1950). Because of superexchange the value of g used may refer to an excited Mn²⁺ state.

Fractional Transition Probabilities of the First Positive Band System ($B^3\Pi \rightarrow A^3\Sigma$) of Molecular Nitrogen

C. E. MONTGOMERY AND R. W. NICHOLLS

Department of Physics, University of Western Ontario, London, Ontario, Canada

(Received March 12, 1951)

AS part of a computational program of fractional vibrational transition probabilities for molecular band systems occurring in upper atmospheric radiations, the results for the first positive system of molecular nitrogen are here presented in Table I.

The method of calculation employed is similar to that used in previously reported results,¹ and involves a computation of the overlap integral of suitably modified hermite wave functions.² It will be noted that the fractional transitional probability $f(v', v'')$ is so defined that in any v' progression

$$\sum_{v''} f(v', v'') = 1.$$

From a 3-dimensional presentation of Table I it will also be noted that what was formerly thought of as the primary Condon parabola in the (v', v'') array of reported intensities of the first positive bands³ is in fact the limbs corresponding to the smaller v'' values of the primary and a subsidiary parabola. The limb of the